

## Article

# Stable Semi-Transparent Dye-Sensitized Solar Modules and Panels for Greenhouse Application

Jessica Barichello <sup>1,\*</sup>, Luigi Vesce <sup>1,\*</sup>, Paolo Mariani <sup>1</sup>, Enrico Leonardi <sup>2</sup>, Roberto Braglia <sup>3</sup>, Aldo Di Carlo <sup>1,4</sup>, Antonella Canini <sup>3</sup> and Andrea Reale <sup>1,\*</sup>

- <sup>1</sup> CHOSE—Centre for Hybrid and Organic Solar Energy, Department of Electronic Engineering, University of Rome “Tor Vergata”, Via del Politecnico 1, 00133 Roma, Italy; jessica.barichello@uniroma2.it (J.B.); paolo.mariani@uniroma2.it (P.M.); aldo.dicarlo@uniroma2.it (A.D.C.)
- <sup>2</sup> Greatcell Solar Italia SRL, Viale Castro Pretorio 122, 00185 Roma, Italy; eleonardi@greatcellsolar.com
- <sup>3</sup> Department of Biology, University of Rome “Tor Vergata”, Via della Ricerca Scientifica 1, 00173 Roma, Italy; roberto.braglia@uniroma2.it (R.B.); canini@uniroma2.it (A.C.)
- <sup>4</sup> ISM-CNR, Istituto di Struttura della Materia, Consiglio Nazionale delle Ricerche, Via del Fosso del Cavaliere 100, 00133 Roma, Italy
- \* Correspondence: vesce@ing.uniroma2.it (L.V.); reale@uniroma2.it (A.R.)

**Abstract:** Our world is facing an environmental crisis that is driving scientists to research green and smart solutions in terms of the use of renewable energy sources and low polluting technologies. In this framework, photovoltaic (PV) technology is one of the most worthy of interest. Dye-sensitized solar cells (DSSCs) are innovative PV devices known for their encouraging features of low cost and easy fabrication, good response to diffuse light and colour tunability. All these features make DSSCs technology suitable for being applied to the so-called agrovoltaic field, taking into account their dual role of filtering light and supporting energy needs. In this project, we used 40 DSSC Z-series connected modules with the aim of combining the devices’ high conversion efficiency, transparency and robustness in order to test them in a greenhouse. A maximum conversion efficiency of 3.9% on a 221 cm<sup>2</sup> active area was achieved with a transparency in the module’s aperture (312.9 cm<sup>2</sup>) area of 35%. Moreover, different modules were stressed at two different temperature conditions, 60 °C and 85 °C, and under light soaking at the maximum power point, showing a strong and robust stability for 1000 h. We assembled the fabricated modules to form ten panels to filter the light from the roof of the greenhouse. We carried out panel measurements in outdoor and greenhouse environments in both sunny and cloudy conditions to find clear trends in efficiency behaviour. A maximum panel efficiency in outdoor conditions of 3.83% was obtained in clear and sunny sky conditions.

**Keywords:** DSSC; panel; stability; outdoor; semi-transparent; module; greenhouse; BIPV; printing



**Citation:** Barichello, J.; Vesce, L.; Mariani, P.; Leonardi, E.; Braglia, R.; Di Carlo, A.; Canini, A.; Reale, A. Stable Semi-Transparent Dye-Sensitized Solar Modules and Panels for Greenhouse Application. *Energies* **2021**, *14*, 6393. <https://doi.org/10.3390/en14196393>

Academic Editor: Jun-ichi Fujisawa

Received: 19 July 2021

Accepted: 29 September 2021

Published: 6 October 2021

**Publisher’s Note:** MDPI stays neutral with regard to jurisdictional claims in published maps and institutional affiliations.



**Copyright:** © 2021 by the authors. Licensee MDPI, Basel, Switzerland. This article is an open access article distributed under the terms and conditions of the Creative Commons Attribution (CC BY) license (<https://creativecommons.org/licenses/by/4.0/>).

## 1. Introduction

Dye-sensitized solar cells (DSSCs) have been a well-known third-generation photovoltaic (PV) technology since M. Grätzel revealed the potential of these devices [1]. In recent years, the interest of scientists has focussed on the device’s structure and on materials optimization in order to increase the power conversion efficiency (PCE) [2–5]. Until now, the maximum PCE has been certified as 13% in small area devices (< 1 cm<sup>2</sup>) [6] and 8.8% in modules of approximately 400 cm<sup>2</sup> of area [7]. Despite these lower efficiencies, if compared to those of the already consolidated semiconductor technologies—around 25% for crystalline silicon (c-Si) and ranging from 14 to 20% for thin film technologies (CdTe, a-Si, CIGS) [6]—DSSCs have been studied for almost 30 years for their peculiar characteristics of transparency and colour versatility, that make them an ideal technology for indoor applications and advanced architectural integration. Natural light viewing is indeed an important parameter for glazing to create a comfortable indoor environment [8]. DSSC technology shows one of the highest transmission rate percentages of solar radiation

amongst TPV (transparent photovoltaic) technologies [9]. With common red and orange dyes, devices have obtained a solar transmission rate of 20–30% [10–12], while through a selected dye system that absorbs light in the ultraviolet and near infrared region, an amazing 60% transmission rate was shown [13]. The typical DSSC's transparency is mainly due to its intrinsic semi-transparent elements. The active layers are embedded between two transparent glasses that face the coated side of a conductive FTO (fluorine-doped tin oxide) layer. On one glass—the photo-electrode (PE)—there is the dye-sensitized TiO<sub>2</sub> layer; on the other glass—the counter-electrode (CE)—there is a platinum layer that works as a catalyst. A liquid electrolyte is sandwiched between the two glasses with the role of dye recharger. This c-Si solar cell technology is not considered suitable for semi-transparent applications because of its intrinsic opacity that does not allow natural light to pass through. Moreover, despite a reduction in price over recent years, silicon wafers still present a significant cost [8,14]. Therefore, research investigated second generation thin films (CdTe, a-Si, CIGS) for PV glazing applications due to their possible semi-transparent design, resulting in more homogeneous daylight in interior spaces compared to that with c-Si solar cells. However, the increase in transparency is at the expense of efficiency, which falls precipitously [15]. Light-induced defects, shortages and materials toxicity have limited their application in building integration. On the contrary, DSSC benefits from low fabrication costs and environmentally friendly components [16].

### 1.1. The Transparency Relevance for Greenhouse PV Application

The DSSC's bifacial transparency and colour tunability allow light entry. Moreover, the dye selection allows choosing of the radiation that passes through [17]. All these characteristics promote this technology as extremely interesting for building integration and semi-transparent applications [16]. In recent works, the feasibility of DSSC applications in greenhouses and its suitability in comparison to other PV technologies has also been discussed [18–21]. With the energy crisis that humanity is facing and the urgent need for use of sustainable energy from renewable sources, 'agrovoltaic' is the coined term to indicate the optimization of land use combining solar PV panels and food crops [22]. For healthy crop growth inside greenhouses there are many controlling systems with different functions, such as regulating temperature, lighting, fans and monitoring devices. As a consequence, the electricity consumed by technologically advanced greenhouses is estimated to be up to 9 KWh/m<sup>2</sup> per year [23]. DSSC technology, with its unique peculiarities, is considered for greenhouse application not only for supporting energy needs but also with the role of selective control of light [19,22,24]. Indeed, DSSC transparency allow the incident light to be filtered, dividing the spectrum between plant growth and electricity production. C-Si technologies have demonstrated success in energy supplies when positioned on greenhouse roofs, but since they have no light transmission, only a portion of the greenhouse may be cultivated [19]. For maximizing light entry, c-Si was placed very high above the crop, increasing greenhouse maintenance costs—but even in this scenario c-Si was incompatible with crops of high economic importance, such as tomatoes, or crops that need 'full sun' conditions [19,25]. Many studies reported a decreased yield in greenhouse cultivation with integrated c-Si for different crops such as French beans, cucumber, wheat, and lettuce [19,26]. These results suggest that c-Si may still have questionable effects on food production. Despite the impressive PCE reached, the new-comer perovskite solar cells (PSK) may find limited use for greenhouse application due to the presence of lead and the consequential environmental effects of degradation of the cells [27]. PSK can however demonstrate high efficiency combined with transparency and long stability over a large area [28]. Different results may be found by using semi-transparent PVs as OPVs and DSSCs [29]. Recently [29,30], pepper plant (*Capsicum annum* L.) growth in a Mediterranean greenhouse has been studied with OPV devices covering 22% of the roof. The experiment compared plant growth under OPV panels and outside under environmental conditions. Shading plants under OPV panels of 25 × 70 cm<sup>2</sup> showed a PCE of 2.1%, and a transparency of 19% produced a better performance in terms of fruit

mass and stem height at the end of season. The shading effect of PV devices protected plants from excessive UV radiation. Roslan et al. [19] have investigated DSSCs' potential in greenhouses. However, few experimental works have demonstrated DSSC application feasibility. Recently, the Irakli group [21] investigated the effect of light filtered by the glass cover in DSSC, comparing it to that of a standard greenhouse. By monitoring the physiological characteristics of the crop, the shading effect of the DSSC cells was evaluated as satisfactory. The crop presented positive results on the qualitative characteristics of the tomato fruits. A recent study focused on creating a proper dye to meet the demand of high PCE and high transparency [31], with the purpose of a greenhouse application. Dessi et al. focused on improving the light absorption capability in the green part of the visible spectrum while maintaining a good transparency in the blue and red regions.

### 1.2. The Role of Filtered Light

The manipulation of light is considered a priority to improve the amount and value of agricultural products. Chlorophyll molecules do not absorb green light and thus this is less important for photosynthesis itself; on the other hand, scientific studies reported that plant development and physiology are strongly influenced by blue or red light. Yorio et al. reported the same amount of dry weight of lettuce grown under blue and red LED light in comparison to lettuce growth under white light [32]. In addition, another study demonstrated the advantages of red light for lettuce growth [33]. Blue light induces biomass production, and the growth of plants irradiated with green light decreases as the proportion of green light increases [34,35]. Besides the electrical support and the benefits from light manipulation, DSSC devices can perform alternative sustainable shading with the aim of reducing the air temperature and regulating the microclimate inside the greenhouse—especially in summertime [36]. Dominiguez, investigating PV application on rooftop surfaces, revealed a significant temperature reduction in comparison to buildings without PV. This effect leads to energy savings for the cooling systems [37]. The same principle works on greenhouses, where the light control requirements are better supported by semi-transparent DSSC devices instead of opaque silicon modules [14]. Garcia et al. have already proved that with the application of external shading by PV systems, the temperature decreased by 9 °C in comparison to the external temperature [38]. PCE, colour and transparency (or light transmittance, LT) are crucial targets to be considered for DSSC application in greenhouses.

### 1.3. Dye Selection

The colour of a DSSC is mainly due to the superposition of the optical spectra of the electrolyte and of the dye, while the transparency is influenced by the TCO (transparent conductive oxide), the dye, the electrolyte, the platinum and the TiO<sub>2</sub> paste formulation (tens or hundreds of nm particle size) and thickness [12]. The selection of the dye is involved in light manipulation for plant growth and energy conversion. Artificial dyes can be divided into two categories: metal–organic dyes, complexes of molecules containing a transition metal, and organic dyes (metal free). Among the organic dyes, D35 (Dyename) is an orange dye considered an excellent choice to see through DSSC devices and can reduce the ruthenium cost. D35 absorbs green light at 500 nm, perfectly matching with the needs of greenhouse harvesting. It does not interfere with the main photosynthetic system, which absorbs in blue (400–420 nm) and red (680–700) regions [39,40]. Aside from its colour characteristics, D35 has shown a significant efficiency of around 5–6%, achieved with a good stability for 1000 h at 85 °C. D35 benefits from a particular D- $\pi$ -A (donor- $\pi$ -acceptor) structure [41–43].

In this work, we covered a 2 m<sup>2</sup> greenhouse area with 40 modules to investigate the trade-off between energy production for an advanced aquaponic greenhouse, and its effect on filtering light for crop growth. The novelty of this work lies on the combination of high PCE, high transparency and strong robustness to thermal and light tests of a DSSC panel for greenhouse application. The champion module (70% aspect ratio) has an efficiency of

3.9% with a transparency of 35% on the module's aperture area (312.9 cm<sup>2</sup>). Moreover, modules showed great stability when stressed for 1000 h at different temperatures (60 and 85 °C) and under light soaking at MPP. The fabricated modules were assembled to form 10 panels, 4 modules each, to cover the whole area inside the greenhouse. We carried out measurements of one panel at different sky conditions—sunny and cloudy—and in different environments—outdoor and inside the greenhouse—obtaining a maximum efficiency of 3.83% with an irradiance of 1 SUN (i.e., 1 kW/m<sup>2</sup>).

## 2. Materials and Methods

In the scale-up process from lab cells (less than 1 cm<sup>2</sup> of active area) to large area devices (more than 10 cm<sup>2</sup> of active area), performances are limited by sheet resistance of the substrate and conditioned by the sealing process of the device [44]. Sheet resistance is faced by printing conducting grids on substrates [45] and by making cells of smaller dimensions connected in various ways [46]. The cells can be either connected in parallel (currents of the cells are summed) or in series (voltages of the cells are summed). There are four possible module structures related to cell interconnections [47]: parallel connection [48], series monolithic [49], series W-type connection [46] and series Z-type connection. The best electric performances were achieved with Z-type structures [50,51]. The advantages of this design are a high voltage output and facility for eventual pre- and post-treatment of the electrodes [52]. Z-connections guarantees uniform and reliable output over large areas in different sun illuminations [53] and temperature conditions [54]. In the Z-type configuration, the DSSM (DSS Module) is composed of identical cells sandwiched between two scribed conducting glass plates, with conducting vertical contacts (typically made of Ag) that connect adjacent cells [51,55]. The main issue of Z-architecture is its effective isolation by sealing of the electrolyte from the vertical connection to avoid the degradation of the silver connections due to chemical reactions. In fact, the rigidity of the vertical interconnects could affect contacts between the upper and lower finger, lowering I<sub>SC</sub> and FF. Indeed, the presence of spikes in the Ag layer, or the volume expansion of the electrolyte [56] could impact the sealing, pushing the electrodes to separate with a subsequent electrolyte leakage [57,58]. To be competitive on the market and to protect all components from environmental contamination, DSSMs are assembled in strings and panels [59]. In 2004, Toyoda et al. connected 64 DSSMs in series to realize a panel [60]. In 2008, a 2 m<sup>2</sup> panel exhibited an efficiency of 6% on an active area at 0.87 sun [61]. Dye solar panels (DSPs) for BIPV (building-integrated photovoltaics) applications were developed on areas of 1.4 m<sup>2</sup> with an efficiency of 3.58% [62] over a whole façade of the École Polytechnique Fédérale–Lausanne (EPFL) campus, Switzerland, as windows [62]. Samsung and Dyepower reported panel demonstrations for BIPV and facade applications [44,62]. All materials involved in the production of DSSMs and panels are commercially available. This aspect fosters a fast development of DSSC technology towards industrialization of DSSC.

The series-connected DSSM fabrication process occurs completely in ambient air. First, glasses were washed with soap to remove organic products and dust; then, they were rinsed in acetone, ethanol and 2-propanol. For each module, two glasses were etched by means of a Nd:YVO<sub>4</sub>, λ = 1064 nm, raster scanning laser in order to isolate 12 cells on them [63] (Figure 1a). The width of the single cell was designed according to well-known compromises between losses in the efficiency of the geometrical area and resistivity of the transparent FTO electrodes [44]. These glasses make up the photoelectrode (PE) and the counter-electrode (CE). On both electrodes, silver contacts were screen-printed and then they were dried at 120 °C for 30 min in an oven [Figure 1b]. On the PE, we printed GreatCell Solar TiO<sub>2</sub> paste (Figure 1c1). After printing, the TiO<sub>2</sub> layer was dried at 120 °C and then sintered at 500 °C for 30 min with a slow increasing ramp temperature. The resulting layer of TiO<sub>2</sub> acting as a wide band-gap semiconductor was 5 μm thick with an approximately 20 nm particle size (Figure 2), in accordance with a TiO<sub>2</sub> layer for semi-transparent application [64].

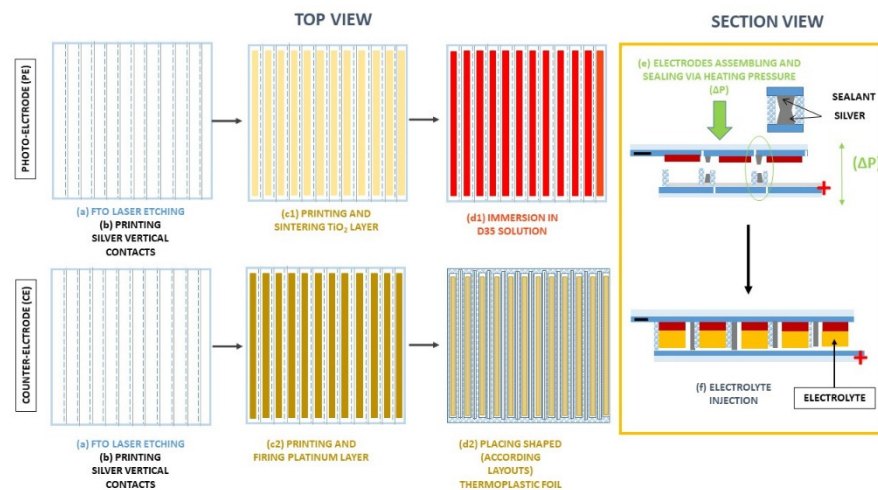


**Figure 1.** Full module assembly. (a–f) module fabrication steps.

On the CE, we screen-printed a Pt paste as a counter electrode, which acts as a catalyst (Figure 1(c2)). The platinum paste was dried at 120 °C and fired at 480 °C for 30 min. Successively, PEs were dipped overnight in a tank for soaking in D35 dye (Figure 1(d1)). The sensitized PEs were removed from the dye bath, rinsed with ethanol and allowed to dry before sealing the PE and CE. The sealing procedure is based on a thermoplastic gasket, with a 80 µm thick Bynel, shaped in accordance with the titanium and silver grid position and melted by a hot press (Figure 1(d2), 1e). The electrolyte was inserted by a vacuum back-filling technique through Bynel-shaped channels at the module edge and then sealed completely (Figure 1f). In our work, the substrate size was 384 cm<sup>2</sup>, with 12 series of connected cells at a 18.46 cm<sup>2</sup> active area each (Figure 3). The 40 DSSC modules were assembled to form DSSC panels. Two serially connected modules with comparable currents, to avoid any performance drop, composed each string (Figure 4a). Two strings were laminated into a panel via a hot vacuum lamination process using an industrial laminator (Laminator Core 2, Rise Technology srl). A low-temperature approach (max temp 85 °C) was developed and adopted to stress the DSSCs modules as little as possible and prevent electrolyte leakage. Two 4 mm-thick tempered glasses were used as external substrates and two 450 µm thick low temperature cross-linking EVA sheets as encapsulants (Figure 4b).

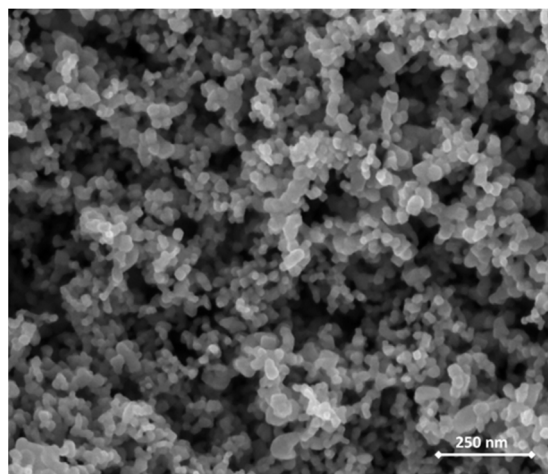


**Figure 2.** SEM image of the TiO<sub>2</sub> layer showing a 20 nm particle size.

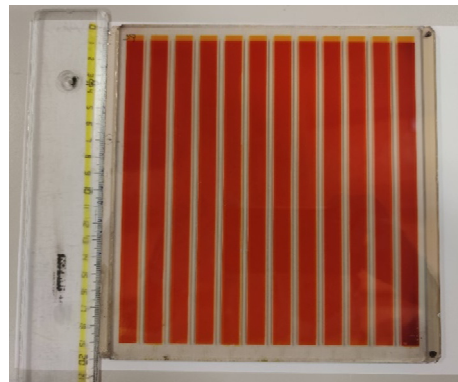


Figure 3. Complete Z-type DSSC module.

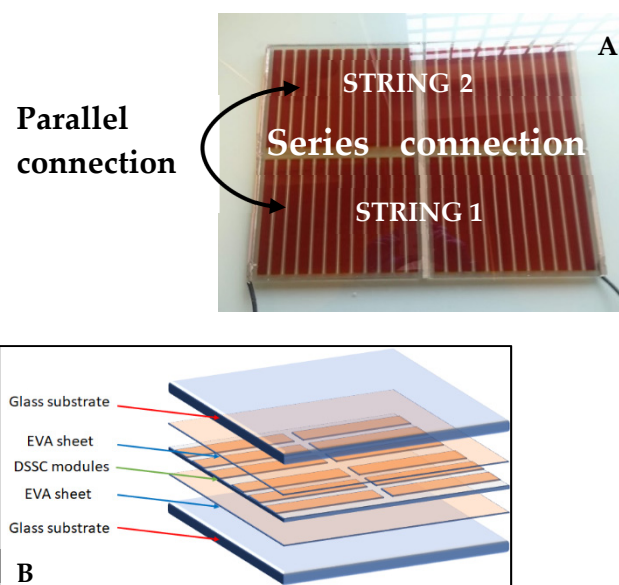


Figure 4. Two serially connected DSSC strings, set in parallel to form a  $4 \times 4$  DSSC panel (A); DSSC panel structure (B).

#### Materials and Facilities

Glass substrates were from Pilkington, at  $7 \Omega/\text{sq}$  and 2.2 mm thick. Etching of substrates was performed using a BrightSolutions, Luce 40 laser. Silver paste for vertical contacts was 7710 from Chimet, while  $\text{TiO}_2$  paste (18 N-RT) and the liquid electrolyte—high stability electrolyte (HSE)—were from GreatCell Solar. The platinum was from 3D Nano. Silver,  $\text{TiO}_2$  and Pt were deposited using a highly automated screen printer (SP) from “Baccini-Applied Materials”. All the drying and sintering processes were performed in an oven, Lenton WHT6/60 (Hope Valley, UK). The thermal stress test was carried out in a Lenton WHT 4/30 oven. The sensitizer—D35 dye (DN-F04)—was from Dyenamo. The thermoplastic material for assembling and sealing the devices was the Bynel (80  $\mu\text{m}$  thick) from Solaronix. Assembling and sealing DSSMs was performed by an automated pneumatic heat press (model 50 speciale from “Memo s.r.l”), composed of two opposite heated plates. External panel substrates were standard tempered 4 mm float glasses. Panel encapsulant was 400  $\mu\text{m}$  low temperature cross-linking EVA from Xinology. Industrial laminator was from Rise technology. The panel frame was made of PETG produced by a Prusa MK3 3D printer. All layer thicknesses were detected by a DektakXT Veeco150 profiometer. Measurements of electrical parameters ( $\text{PCE}$ ,  $I_{\text{SC}}$ ,  $V_{\text{OC}}$  and FF) were carried out under a class B sun simulator (Solar Constant 1200 KHS) in ambient air/room temperature at AM 1.5G,  $100 \text{ mW cm}^{-2}$ , calibrated using a Keithley 2420 as a source-meter at ambient

conditions, calibrated with a SKS 1110 sensor (Skye instruments Ltd.). An “Arkeo” light soaker (from CICCI research) was used for the light soaking test (CICCI Research). The transmittance spectra were carried out by an MPC-2200 (SHIMADZU).

### 3. Results and Discussion

#### 3.1. PV Module Performances

In Figure 5, the electrical parameters (PCE,  $I_{SC}$ , FF and  $V_{OC}$ ) of the 40 modules are shown. Statistics are summarized in Table 1. The following measurements were detected on the first day of fabrication of each device. The average PCE was around 2.5%, the average voltage was equal to 8.9 V and the average current reached 152 mA.

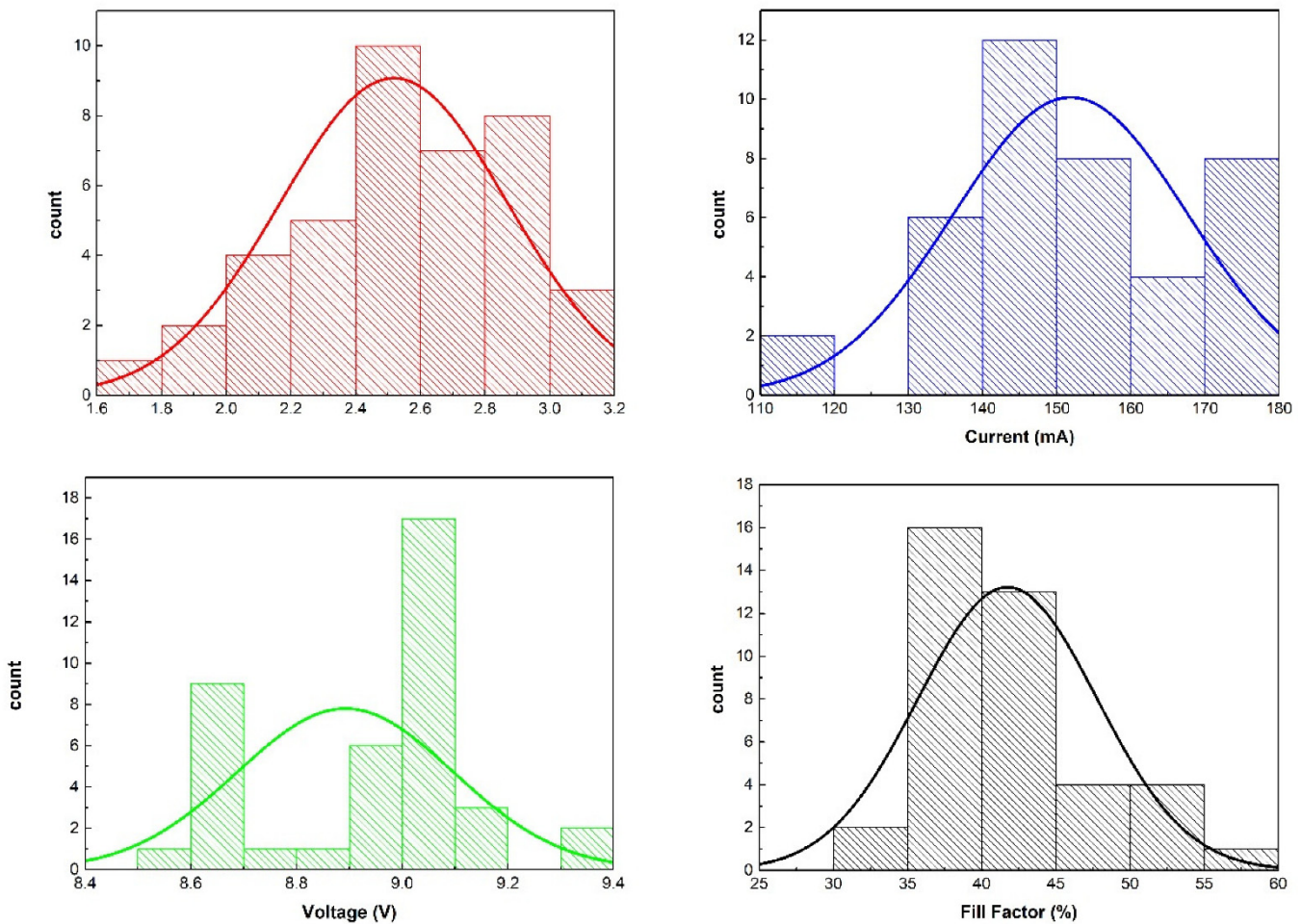


**Figure 5.** Distribution of electrical parameters of 40 modules made for the Aquaponic Easy Farm project. Clockwise: PCE,  $I_{SC}$ ,  $V_{OC}$  and F.

**Table 1.** Average values and standard deviation of the electrical parameters of the 40 modules.

PCE Average (%)	Current Average (mA)	Voltage Average (V)	FF Average (%)
$2.5 \pm 0.4$	$152 \pm 16$	$8.9 \pm 0.2$	$41.7 \pm 1.1$

Since we adopted a series connection, the calculated voltage for each cell is 0.75 V, perfectly in agreement with the reported results in the literature for small area devices with D35 dye [42,43]. The  $J_{sc}$  is  $9 \text{ mA/cm}^2$ , lower compared to the data available in the literature on small area devices:  $12 \text{ mA/cm}^2$ . This loss of current is attributed to the absence, in this structure, of the scattering layer [53]. The scattering layer cannot be applied in DSSC for greenhouse application because it would significantly lower the transparency of the

device [65]. In Figure 6, the graph represents the normalized efficiency of a module as built. Efficiency starts from a value equal to 2.5%. During the following days, efficiency improved constantly until it reached an increase of around 30% from the starting efficiency, after 800 h. At 1800 h after manufacture, on visual inspection, the module did not show traces of delamination or silver grid corrosion. Typically, in DSSC technology the best efficiencies are observed after several days after the device manufacture. In particular, increases in the FF parameter, due to an improved interaction between the electrolytic species (tri-iodide/iodide) and the mesoporous structure in which dye is anchored [52]. Indeed, during this time, the liquid electrolyte keeps buffering and so filling the pores of the  $\text{TiO}_2$ , fostering the improvement of reactions with the dye. The built module, measured according to shelf-life conditions (ISOS-D-1) [66], increased the PCE after some days, as shown in Figure 6—showing a very large increment in PCE (+29%), mainly due to the FF (+27%). By the simple mathematical procedure presented in a previous paper by Calogero et al. [67], we estimated that our module produced during the entire shelf-life test (1800 h), considering the lowest current, a battery capacity of 489 Ah, corresponding approximately to the capacity of more than 300 type AAA alkaline standard batteries at 1200 mAh at the same time.

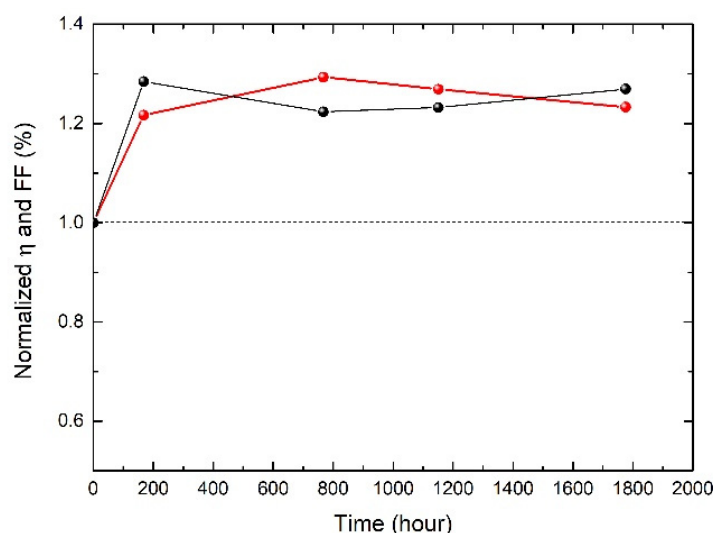


**Figure 6.** Shelf-life conditions (ISOS-D-1) of a DSSC module. The red line represents the PCE and the black line the FF.

### 3.2. Stability Test

Certification tests are useful for assessing stability and to ensure a reliable use of new technologies [42]. Certification protocols related to DSSC technology are not present in the literature, but ISOS-D-2 protocols [64], IEC 61215, JIS C8938 and JIS C8991 can be widely used for this scope [68].

We performed a thermal stress at 60 °C in the dark, a thermal stress test at 85 °C in the dark and a light soaking at room temperature at MPP (i.e., continuously illuminated by an optical source equivalent to 1 Sun; ISOS-L-1 [66]). In Figure 7, we report the stability graph of the three modules that have undergone the three different tests for 1000 h. All modules successfully passed the stability tests, with losses lower than 20% of efficiency. The module at 60 °C in the dark increased its efficiency by 25% up from its starting PCE during the first 200 h; then remained stable until the end of 1000 h with no sign of deterioration. The module under constant illumination boosted its PCE during the first 200 h up to 10% compared to the starting efficiency, then, the PCE started to drop, with losses of less than 20% compared to the initial PCE. At 85 °C, the tested modules have shown PCE drop after 1000h of lower than 12% compared to the initial value (Figure 7).

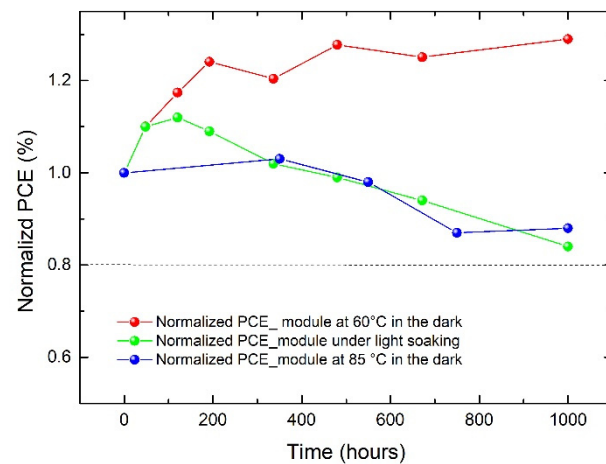


**Figure 7.** 1000 h test at two different temperatures (60 °C and 85 °C) and under light soaking at environmental temperature.

We reported in Figure 8 the best efficiency of 3.88% (+29% from the starting PCE) at the end of the 60 °C test in the dark. The increase in the DSSC device's performance at 60 °C in the oven is well known and already proven in small area cells by several groups [69,70]. The increment in the temperature leads to a reduction in electrolyte viscosity so it can better penetrate into TiO<sub>2</sub> pores. Moreover, the ionic diffusion improves and, consequently, the dye experiences faster chemical reduction, boosting the FF and the current, as it is possible to notice in Figure 9A, and also at 85 °C in Figure 9B. At 60 °C, the FF showed an increase of 16% from the starting value, increasing until the end of test, while the current had a slighter improvement up to 6%. At 85 °C, we can notice the beneficial effects of the temperature during the first 350 h, where the current value was boosted by 6% and the FF reached +3%. At 60 °C, the V<sub>oc</sub> had a flat trend; on the contrary, at 85 °C the voltage had a constant drop, reaching −10% from the starting value. All these results are perfectly in accordance with electrical parameter trends already presented in the literature [71].

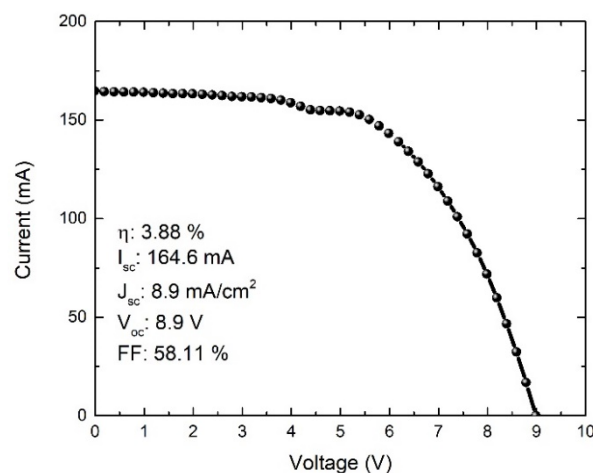


**Figure 8.** IV curve of the best PCE at 60 °C.

Given the right combination choice of dye and electrolyte to avoid dye desorption, platinum dissolution or iodine consumption in electrolytes [72], these tests proved the reliability of the fabricated module. Monitoring the FF on all thermal and light tests (Figure 9A–C), no drops can be observed, meaning that the sealing and the interconnection electrodes have also preserved their functionality in stress conditions [70,73].

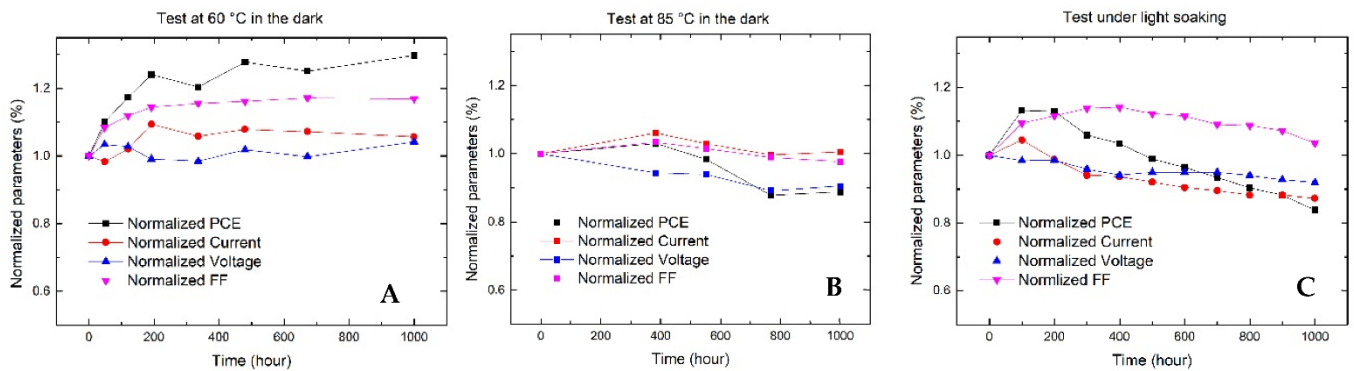


Figure 9. Trend of all electrical parameters during the 1000 h test (A) at 60 °C, (B) at 85 °C and (C) under light soaking.

### 3.3. Transparency

We report the transmittance measurements in Figure 10. Transparency was calculated on each individual section of the module (see Table 2), based on Equation (1) [65], where  $D_\lambda$  represents the incident light distribution,  $\tau(\lambda)$  the transmittance values of the illuminated object,  $V(\lambda)$  the sensitivity factor of the human eye, and  $\lambda$  the wavelength. The overall transparency of the module was then obtained through Equation (2), which allows the taking into account of the presence of the silver grids. The transparency value of the form,  $\tau_{module}$ , was found to be 35%.

$$\tau_v = \frac{\sum_{\lambda=380}^{780} D_\lambda \tau(\lambda) V(\lambda) \Delta\lambda}{\sum_{\lambda=380}^{780} D_\lambda V(\lambda) \Delta\lambda} \tag{1}$$

$$\tau_{module} = \frac{(\tau_{glass} A_{glass}) + (\tau_{cell} A_{cell}) + (\tau_{Ag} A_{Ag})}{Substrate Area} \tag{2}$$

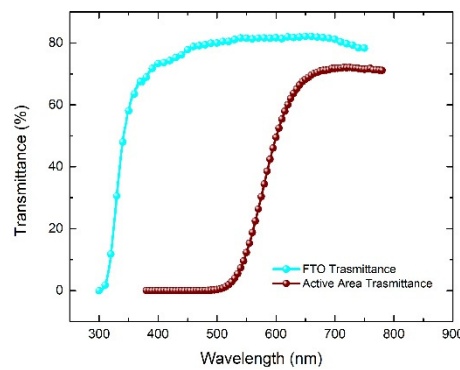


Figure 10. Glass substrate and module transmittance.

Table 2. Transmittance values of the various components of the module and relative area in cm<sup>2</sup>.

Module Section	Transmittance	Area (cm <sup>2</sup> )
Active Area	24%	221.52
Glass	78%	71.36
Silver grids	0%	20.02

### 3.4. PV Panel Performances

The panel was characterized in outdoor and in greenhouse environments in both sunny and cloudy conditions. We present the overall IV curves, with the efficiency evalu-

ated in different configurations (horizontal and  $45^\circ$  tilted facing perpendicularly the sun, Figure 11), to compare the outdoor behaviour to the performance inside the greenhouse in both weather conditions (Figure 12). We collected precise measurements of solar radiation at the meteorological outdoor station ESTER–University of Rome ‘Tor Vergata’; in sunny conditions, on 20 May 2021 in Rome at 1 p.m. CEST (Central European Summer Time), the calculated irradiation was 1 SUN; in cloudy conditions, on 14 May 2021 in Rome at 1 p.m. CEST time, it was 0.075 SUN. On Table 3, the electrical parameters are shown.

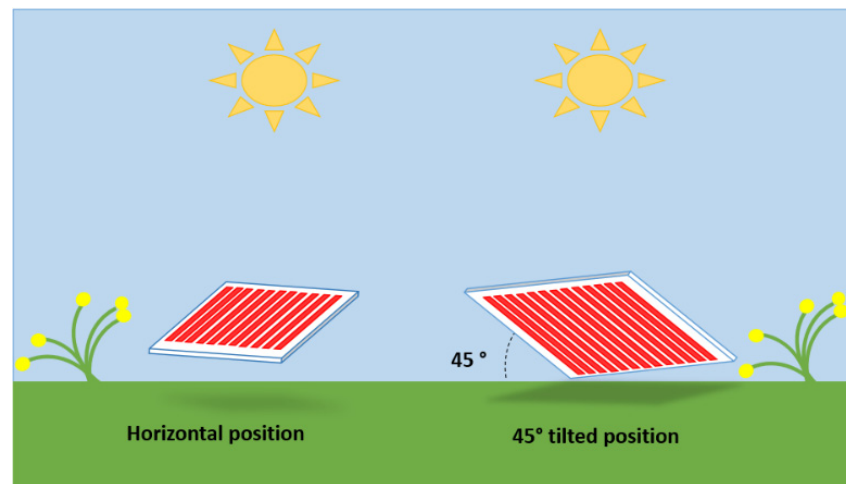


Figure 11. Measuring position.

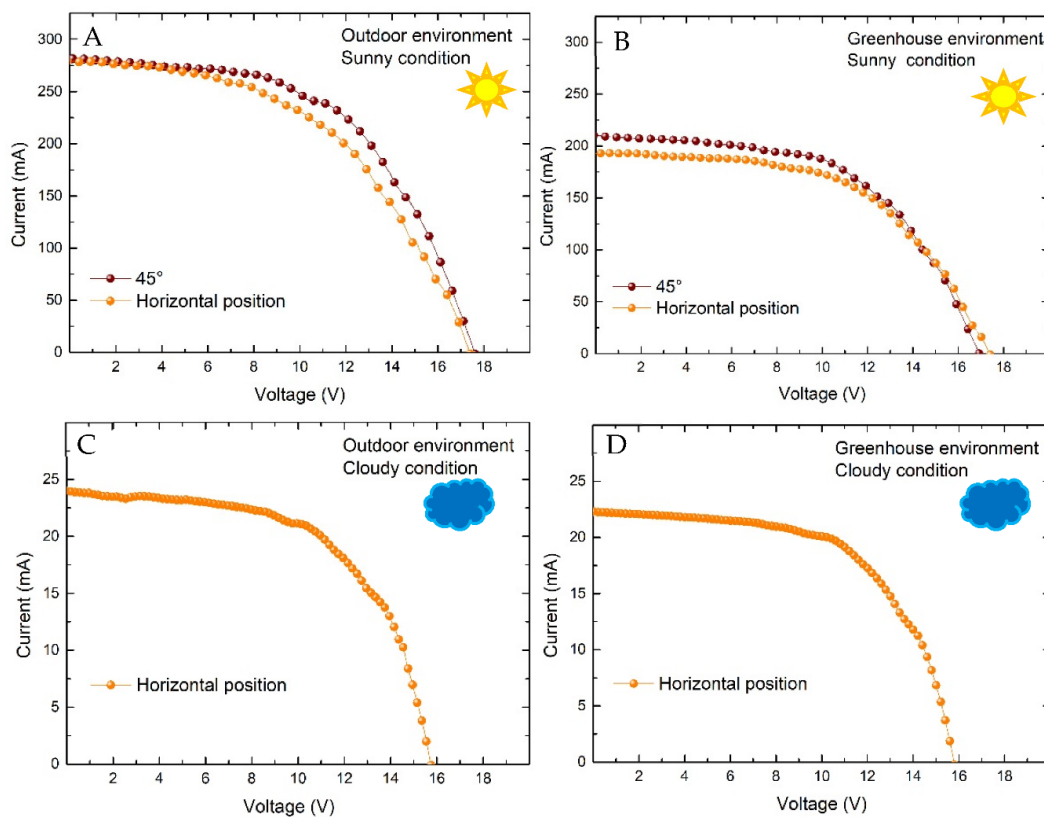


Figure 12. (A): IV in sunny and clear conditions, outdoor environment. (B): IV in sunny and clear conditions, greenhouse environment. (C): IV cloudy conditions, outdoor environment. (D): IV cloudy conditions, greenhouse environment.

**Table 3.** Electrical parameters of the DSSC panel at different meteorological conditions and environments. Panel's active area: 886 cm<sup>2</sup>.

SUNNY CONDITION, Outdoor	P max (W)	Isc (mA)	Voc (V)	FF (%)	PCE (%)
45°	2.7	281.26	17.6	54.7	3.05
Horizontal	2.4	278.98	17.4	49.6	3.83
SUNNY CONDITION, Greenhouse					
45°	1.94	210.28	16.9	54.5	2.18
Horizontal	1.8	192.44	16.9	54.8	2.94
CLOUDY CONDITION, Outdoor					
Horizontal	0.22	23.98	15.7	58.4	4.62
CLOUDY CONDITION, Greenhouse					
Horizontal	0.2	22.3	15.8	59.8	4.42

The efficiency was evaluated with consideration of the normalized irradiance corresponding to the different orientations of the panel with respect to the solar radiation [54]. The best efficiency of 3.83% was obtained in the outdoor environment, with sunny conditions (Table 3). In cloudy conditions, the majority of the irradiation was attributed to diffuse light, and we considered only the horizontal positions as a reference for the greenhouse application. DSSC devices work better at low irradiation intensities; the electrolyte can completely reduce the oxidized dye and consequently the fill factor increases, without limitations in the diffusion of redox species. The obtained voltage is perfectly in agreement with the module electrical parameters and panel structure. The voltage of one string is the sum of the voltage from two series of connected modules. Considering that, the modules had a voltage of around 9 Volts (Table 1) and panel voltages showed values between 15 and 17 Volts under different conditions. The total panel current is the sum of the outgoing current from the two strings. Additionally, in this case, the panel current (Table 3, 281 mA measured under optimum solar conditions at 1 SUN), matches with the average current of 152 mA (1 SUN) shown in Table 1 for a single module. At the end, the fabricated panels were installed in a greenhouse (Figure 13) on top of plant cultivations for further studies based on plant growth in relation to the filtered light.



**Figure 13.** (A) DSSC panels in the Aquaponic greenhouse. The panel frame has been designed and produced using a recyclable PET material via 3D printing. (B) Lettuce plants at the beginning of the experimentation and (C) lettuce plants grown under panels after 42 days.

#### 4. Conclusions

In the “Aquaponic Easy Farm 4.0” project, of the Lazio Region, Italy, we worked on the production of two square meters of photovoltaic panel to be applied inside an Aquaponic greenhouse. In this study, we focused on the development of the panels with consideration of the two main parameters for a photovoltaic device inside a greenhouse: transparency and efficiency. We chose DSSC technology for its peculiar characteristic of high ratio between transparency and efficiency, extensively discussed in the introduction. We carefully described the ambitious and demanding engineering procedure of Z-type module and panel fabrication in order to obtain efficient, transparent and stable devices. We measured a module for 1800 h under shelf-life conditions. Modules were deeply stressed under light at high temperatures, retaining at least 80% of their original efficiency after the stress tests. We obtained a maximum PCE of 3.88% in a single module and a transparency of 35% on the aperture area (312.9 cm<sup>2</sup>). Moreover, the modules survived fruitfully in the 60 °C test, showing an increment in the PCE after 1000 h; no significant drops were detected on tested modules at 85 °C or under light. At the end, we assembled a panel with 4 modules obtaining a maximum efficiency of 3.83% in sunny conditions in an outdoor environment. The panel presents a voltage between 16–18 Volts and a power capacity between 2–3 Watts that can supply part of the energy needs in a greenhouse for temperature and humidity sensors. Preliminary results concerning plant growth under filtered light from DSSCs suggest no differences between the growth of lettuce under natural and DSC-filtered light. Further studies will be the subject of a forthcoming report on plant growth in the DSC greenhouse environment.

**Author Contributions:** Conceptualization, A.R. and A.C.; methodology, L.V., P.M., J.B., A.R. and E.L.; validation, A.R., L.V., J.B. and P.M.; formal analysis, J.B., L.V., P.M. and A.R.; investigation, J.B., L.V., P.M., E.L. and A.R.; resources, A.R., A.C., R.B. and A.D.C.; data curation, J.B.; writing—original draft preparation, J.B.; writing—review and editing, L.V., P.M., A.R., J.B. and E.L.; visualization, J.B., L.V., P.M. and A.R.; supervision, A.R.; project administration, A.R., R.B. and A.C.; funding acquisition, A.R. and A.C. All authors have read and agreed to the published version of the manuscript.

**Funding:** This research was funded by Regione Lazio, POR FESR LAZIO 2014-2020, project name “Aquaponic easy farm 4.0”, project code A0206E0090, and project “COPPER—Celle solari polimeriche per applicazioni agrovoltatiche in ortoflorovivaismo” by Regione Lazio (Progetto di Gruppo di Ricerca—L.R. Lazio 13/08 n. 85-2017-15266).

**Institutional Review Board Statement:** Not applicable.

**Informed Consent Statement:** Not applicable.

**Data Availability Statement:** The data presented in this study are available on request from the corresponding authors.

**Acknowledgments:** We acknowledge the helpful discussion with Cristina Cornaro; ESTER meteorological outdoor station, University of Rome ‘Tor Vergata’, and the following companies: Digital Cooking, Agri Island, App To You and ORION Meccanica.

**Conflicts of Interest:** The authors declare no conflict of interest.

#### References

1. O’Reagan, B.; Grätzel, M. A low-cost, high-efficiency Solar-Cell based on Dye-Sensitized Colloidal TiO<sub>2</sub> films. *Nature* **1991**, *353*, 737–740. [\[CrossRef\]](#)
2. Gong, J.; Sumathy, K.; Qiao, Q.; Zhou, Z. Review on dye-sensitized solar cells (DSSCs): Advanced techniques and research trends. *Renew. Sustain. Energy Rev.* **2017**, *68*, 234–246. [\[CrossRef\]](#)
3. Shakeel Ahmada, M.; Pandeya, A.K.; Abd Rahima, N. Advancements in the development of TiO<sub>2</sub> photoanodes and its fabrication methods for dye sensitized solar cell (DSSC) applications. A review. *Renew. Sustain. Energy Rev.* **2017**, *77*, 89–108. [\[CrossRef\]](#)
4. Selvaraj, P.; Roy, A.; Ullah, H.; Devi, P.S.; Tahir, A.A.; Mallick, T.K.; Sundaram, S. Soft-template synthesis of high surface area mesoporous titanium dioxide for dye-sensitized solar cells. *Int.J. Energy Res.* **2019**, *43*, 523–524. [\[CrossRef\]](#)
5. Ullah, H.; Bibi, S.; Tahir, A.; Mallick, T.K. Donor-acceptor polymer for the design of All-Solid-State dye-sensitized solar cells. *J. Alloy. Compd.* **2017**, *696*, 914–922. [\[CrossRef\]](#)

6. NREL Site. Available online: <https://www.nrel.gov/pv/cell-efficiency.html> (accessed on 25 June 2021).
7. Green, M.A.; Dunlop, E.D.; Hohl-Ebinger, J.; Yoshita, M.; Kopidakis, N.; Ho-Baillie, A.W.Y. Solar cell efficiency tables (Version 55). *Prog. Photovolt. Res. Appl.* **2020**, *28*, 3–15. [[CrossRef](#)]
8. Selvaraj, P.; Ghosh, A.; Mallick, T.K.; Sundaram, S. Investigation of semi-transparent dye-sensitized solar cells for fenestration integration. *Renew. Energy* **2019**, *141*, 516–525. [[CrossRef](#)]
9. Pulli, E.; Rozzi, E.; Bella, F. Transparent photovoltaic technologies: Current trends towards upscaling. *Energy Convers. Manag.* **2020**, *219*, 112982. [[CrossRef](#)]
10. Ren, Y.; Sun, D.; Cao, Y.; Tsao, H.N.; Yuan, Y.; Zakeeruddin, S.M.; Wang, P.; Grätzel, M. A Stable Blue Photosensitizer for Color Palette of Dye-Sensitized Solar Cells Reaching 12.6% Efficiency. *J. Am. Chem. Soc.* **2018**, *140*, 2405–2408. [[CrossRef](#)]
11. Otaka, H.; Kira, M.; Yano, K.; Ito, S.; Mitekura, H.; Kawata, T.; Matsui, F. Multi-colored dye-sensitized solar cells. *J. Photochem. Photobiol. A Chem.* **2004**, *164*, 67–73. [[CrossRef](#)]
12. Selvaraj, P.; Baig, H.; Mallick, T.K.; Siviter, J.; Montecucco, A.; Li, W.; Paul, M.; Sweet, T.; Gao, M.; Knox, A.R.; et al. Enhancing the efficiency of transparent dye-sensitized solar cells using concentrated light. *Sol. Energy Mater. Sol. Cells* **2018**, *175*, 29–34. [[CrossRef](#)]
13. Zhang, K.; Qin, C.; Yang, X.; Islam, A.; Zhang, S.; Chen, H.; Han, L. High-Performance, transparent, dye-sensitized solar cells for see-through photovoltaic windows. *Adv. Energy Mater.* **2014**, *4*, 1301966. [[CrossRef](#)]
14. Biyik, E.; Araz, M.; Hepbasli, A.; Shahrestani, M.; Yao, R.; Shao, L.; Essah, E.; Oliveira, A.; del Caño, T.; Rico, E.; et al. A key review of building integrated photovoltaic (BIPV) systems. *Eng. Sci. Technol. Int. J.* **2017**, *20*, 833–858. [[CrossRef](#)]
15. Skandalos, N.; Karamanis, D. PV glazing technologies. *Renew. Sustain. Energy Rev.* **2015**, *49*, 306–322. [[CrossRef](#)]
16. Parisi, M.L.; Maranghi, S.; Vesce, L.; Sinicropi, A.; di Carlo, A.; Basosi, R. Prospective life cycle assessment of third-generation photovoltaics at the pre-industrial scale: A long-term scenario approach. *Renew. Sustain. Energy Rev.* **2020**, *121*, 109703. [[CrossRef](#)]
17. Hagfeldt, A.; Boschloo, G.; Sun, L.; Kloo, L.; Pettersson, H. Dye-Sensitized Solar Cells. *Chem. Rev.* **2010**, *110*, 6595–6663. [[CrossRef](#)]
18. Chalkias, D.A.; Charalampopoulos, C.; Aivali, S.; Andreopoulou, A.K.; Karavoti, A.; Stathatos, E. A Di-Carbazole-Based Dye as a Potential Sensitizer for Greenhouse-Integrated Dye-Sensitized Solar Cells. *Energies* **2021**, *14*, 1159. [[CrossRef](#)]
19. Roslan, N.; Ya'acob, M.E.; Radzi, M.A.M.; Hashimoto, Y.; Jamaludin, D.; Chen, G. Dye Sensitized Solar Cell (DSSC) greenhouse shading: New insights for solar radiation manipulation. *Renew. Sustain. Rev.* **2018**, *92*, 171–186. [[CrossRef](#)]
20. Allardyce, C.S.; Fankhauser, C.; Zakeeruddin, S.M.; Grätzel, M.; Dyson, P.J. The influence of greenhouse-integrated photovoltaics on crop production. *Sol. Energy* **2017**, *155*, 517–522. [[CrossRef](#)]
21. Ntinias, G.K.; Kadoglidou, K.; Tselivika, N.; Krommydas, K.; Kalivas, A.; Ralli, P.; Irakli, M. Performance and Hydroponic Tomato Crop Quality Characteristics in a Novel Greenhouse Using Dye-Sensitized Solar Cell Technology for Covering Material. *Horticulturae* **2019**, *5*, 42. [[CrossRef](#)]
22. Dupraz, C.; Marrou, H.; Talbot, G.; Dufour, L.; Nogier, A.; Ferard, Y. Combining solar photovoltaic panels and food crops for optimising land use: Towards new agrivoltaic schemes. *Renew. Energy* **2011**, *36*, 2725–2732. [[CrossRef](#)]
23. Campiotti, C.; Dondi, F.; Genovese, A.; Alonzo, G.; Catanese, V.; Incrocci, L.; Bibbiani, C. Photovoltaic as sustainable Energy for greenhouse and closed plant production system. *Acta Hort.* **2008**, *797*, 373–378. [[CrossRef](#)]
24. Narra, V.K.; Ullah, H.; Singh, V.K.; Giribabu, L.; Senthilarasu, S.; Karazhanov, S.Z.; Tahir, A.A.; Mallick, T.K.; Upadhyay, H.M. D- $\pi$ -A system based on zinc porphyrin dyes for dye-sensitized solar cells: Combined experimental and DFT-TDDFT study. *Polyhedron* **2015**, *100*, 313–320. [[CrossRef](#)]
25. Ureña-Sánchez, R.; Callejón-Ferre, Á.J.; Pérez-Alonso, J.; Carreño-Ortega, Á. Greenhouse tomato production with electricity generation by roof-mounted flexible solar panels. *Sci. Agric.* **2012**, *69*, 233–239. [[CrossRef](#)]
26. Marrou, H.; Wéry, J.; Dufour, L.; Dupraz, C. Productivity and radiation use efficiency of lettuces grown in the partial shade of photovoltaic panels. *Eur. J. Agron.* **2013**, *44*, 54–66. [[CrossRef](#)]
27. Babayigit, A.; Ethirajan, A.; Muller, M.; Conings, B. Toxicity of organometal halide perovskite solar cells. *Nat. Mater.* **2016**, *15*, 247–251. [[CrossRef](#)]
28. Subhani, W.S.; Wang, K.; Du, M.; Wang, X.; Yuan, N.; Ding, J.; Liu, S. Anti-solvent engineering for efficient semitransparent CH<sub>3</sub>NH<sub>3</sub>PbBr<sub>3</sub> perovskite solar cells for greenhouse applications. *J. Energy Chem.* **2019**, *34*, 12–19. [[CrossRef](#)]
29. La Notte, L.; Giordano, L.; Calabrò, E.; Bedini, R.; Colla, G.; Puglisi, G.; Reale, A. Hybrid and organic photovoltaics for greenhouse applications. *Appl. Energy* **2020**, *278*, 115582. [[CrossRef](#)]
30. Zisis, C.; Pechlivani, E.M.; Tsimikli, S.; Mekeridis, E.; Laskarakis, A.; Logothetidis, S. Organic Photovoltaics on Greenhouse Rooftops: Effects on Plant Growth. *Mater. Today Proc.* **2019**, *19*, 65–72. [[CrossRef](#)]
31. Dessì, A.; Calamante, M.; Sinicropi, A.; Parisi, M.L.; Vesce, L.; Mariani, P.; Taheri, B.; Ciocca, M.; Di Carlo, A.; Zani, L.; et al. Thiazolo [5,4-d] thiazole-based organic sensitizers with improved spectral properties for application in greenhouse-integrated dye-sensitized solar cells. *Sustain. Energy Fuels* **2020**, *4*, 2309–2321. [[CrossRef](#)]
32. Yorio, N.C.; Goins, G.D.; Kagie, H.R.; Wheeler, R.M.; Sager, J.C. Improving Spinach, Radish, and Lettuce Growth under Red Light Emitting Diodes (LEDs) with Blue Light Supplementation. *HortScience* **2001**, *36*, 380–383. [[CrossRef](#)]
33. Kim, J.; Kang, M.; Kwak, O.K.; Yoon, Y.; Min, K.S.; Chu, M. Fabrication and Characterization of Dye-Sensitized Solar Cells for Greenhouse Application. *Int. J. Photoenergy* **2014**, *2014*, 1–7. [[CrossRef](#)]
34. McNellis, T.W.; Deng, X.W. Light control of seedling morphogenetic pattern. *Plant Cell* **1995**, *7*, 1749–1761.

35. Kim, H.H.; Goins, G.D.; Wheeler, R.M.; Sager, J.C. Stomatal conductance of lettuce grown under or exposed to different light quality. *Ann. Bot.* **2004**, *94*, 691–697. [[CrossRef](#)]
36. Lu, L.; Ya'acob, M.E.; Anuar, M.S.; Chen, G.; Othman, M.H.; Iskandar, A.N.; Roslan, N. Thermal analysis of a portable DSSC mini greenhouse for botanical drugs cultivation. *Energy Rep.* **2020**, *6*, 238–253. [[CrossRef](#)]
37. Dominguez, A.; Kleiss, J.; Luvall, J.C. Effect of solar photovoltaic panels on roof heat transfer. *Sol. Energy* **2011**, *85*, 2244–2255. [[CrossRef](#)]
38. Garcia, M.L.; Medrano, E.; Sanchez-Guerrero, M.C.; Lorenzo, P. Climatic effects of two cooling systems in greenhouses in the Mediterranean area: External mobile shading and fog system. *Biosyst. Eng.* **2011**, *108*, 133–143. [[CrossRef](#)]
39. Leandri, V.; Ellis, H.; Gabrielsson, E.; Sun, L.; Boschloo, G.; Hagfeldt, A. Organic hydrophilic dye for water-based dyesensitized solar cells. *Phys. Chem. Chem. Phys.* **2014**, *16*, 19964–19971. [[CrossRef](#)] [[PubMed](#)]
40. Vamvounis, G.; Glasson, C.R.; Bieske, E.J.; Dryza, V. Modulating electron injection from an organic dye to a titania nanoparticle with a photochromic energy transfer acceptor. *J. Mater. Chem. C* **2016**, *4*, 6215. [[CrossRef](#)]
41. Hagberg, D.P.; Jiang, X.; Gabrielsson, E.; Linder, M.; Marinado, T.; Brinck, T.; Hagfeldt, A.; Sun, L. Symmetric and unsymmetric donor functionalization. comparing structural and spectral benefits of chromophores for dye-sensitized solar cells. *J. Mater. Chem.* **2009**, *19*, 7232–7238. [[CrossRef](#)]
42. Jiang, X.; Marinado, T.; Gabrielsson, E.; Hagberg, D.P.; Sun, L.; Hagfeldt, A. Structural Modification of Organic Dyes for Efficient Coadsorbent-Free Dye-Sensitized Solar Cells. *J. Phys. Chem. C* **2010**, *114*, 2799–2805. [[CrossRef](#)]
43. Perganti, D.; Giannouri, M.; Kontos, A.G.; Falaras, P. Cost-efficient platinum-free DSCs using colloidal graphite counter electrodes combined with D35 organic dye and cobalt (II/III) redox couple. *Electrochim. Acta* **2017**, *232*, 517–527. [[CrossRef](#)]
44. Vesce, L.; Guidobaldi, A.; Mariani, P.; di Carlo, A.; Parisi, M.L.; Maranghi, S.; Baso, R. Scaling-up of Dye Sensitized Solar Modules. In *World Scientific Reference of Hybrid Materials*; World Scientific: Singapore, 2019; pp. 423–485.
45. Ramasamy, E.; Lee, W.J.; Lee, D.Y.; Song, J.S. Portable, parallel grid dye-sensitized solar cell module prepared by screen printing. *J. Power Sources* **2007**, *165*, 446–449. [[CrossRef](#)]
46. Zhang, J.; Lin, H.; Li, J.B.; Li, X.; Zhao, X.C. DSCs Modules Fabricated by Screen Printing. *Key Eng. Mater.* **2010**, *434–435*, 638–641. [[CrossRef](#)]
47. Mariani, P.; Vesce, L.; di Carlo, A. The role of printing techniques for large-area dye sensitized solar cells. *Semicond. Sci. Technol.* **2015**, *30*, 104003. [[CrossRef](#)]
48. Dai, S.; Wang, K.; Weng, J.; Sui, Y.; Huang, Y.; Xiao, S.; Chen, S.; Hu, L.; Kong, F.; Pan, X.; et al. Design of DSC panel with efficiency more than 6%. *Sol. Energy Mater. Sol. Cells* **2005**, *85*, 447–455. [[CrossRef](#)]
49. Takeda, Y.; Kato, N.; Higuchi, K.; Takeichi, A.; Motohiro, T.; Fukumoto, S.; Sano, T.; Toyoda, T. Monolithically series-interconnected transparent modules of dye-sensitized solar cells. *Sol. Energy Mater. Sol. Cells* **2009**, *93*, 808–811. [[CrossRef](#)]
50. Fukui, A.; Fuke, N.; Komiya, R.; Koide, N.; Yamanaka, R.; Katayama, H.; Han, L. Dye-Sensitized Photovoltaic Module with Conversion Efficiency of 8.4%. *Appl. Phys. Express* **2009**, *2*, 082202. [[CrossRef](#)]
51. Giordano, F.; Guidobaldi, A.; Petrolati, E.; Vesce, L.; Riccitelli, R.; Reale, A.; Brown, T.M.; di Carlo, A. Realization of high performance large area Z-series-interconnected opaque dye solar cell modules. *Prog. Photovoltaics Res. Appl.* **2013**, *21*, 1653–1658. [[CrossRef](#)]
52. Iftikhar, H.; Sonai, G.G.; Hashmi, S.G.; Nogueira, A.F.; Lund, P.D. Progress on Electrolytes Development in Dye-Sensitized Solar Cells. *Materials* **2019**, *12*, 1998. [[CrossRef](#)] [[PubMed](#)]
53. Vesce, L.; Riccitelli, R.; Soscia, G.; Brown, T.M.; di Carlo, A.; Reale, A. Optimization of nanostructured titania photoanodes for dye-sensitized solar cells: Study and experimentation of TiCl<sub>4</sub> treatment. *J. Non-Cryst. Solids* **2010**, *356*, 1958–1961. [[CrossRef](#)]
54. Reale, A.; Cinà, L.; Malatesta, A.; de Marco, R.; Brown, T.M.; di Carlo, A. Estimation of Energy Production of Dye-Sensitized Solar Cell Modules for Building-Integrated Photovoltaic Applications. *Energy Technol.* **2014**, *2*, 531–541. [[CrossRef](#)]
55. Sastrawana, R.; Beier, J.; Belledina, U.; Hemming, S.; Hinsch, A.; Kernd, R.; Vetter, C.; Petrate, F.M.; Prodi-Schwabe, A.; Lechner, P.; et al. A glass frit-sealed dye solar cell module with integrated series connections. *Sol. Energy Mater. Sol. Cells* **2006**, *90*, 1680–1691. [[CrossRef](#)]
56. Giordano, F.; Petrolati, E.; Brown, T.M.; Reale, A.; di Carlo, A. Series-connection designs for dye solar cell modules. *IEEE Trans. Electron Devices* **2011**, *58*, 2759–2764. [[CrossRef](#)]
57. Han, C.; Park, S.; Oh, W. Reliability-based structural optimization of 300 × 300 mm<sup>2</sup> dye-sensitized solar cell module. *Sol. Energy* **2017**, *150*, 128–135. [[CrossRef](#)]
58. Mariani, P.; Agresti, A.; Vesce, L.; Pescetelli, S.; Palma, A.L.; Tomarchio, F.; Karagiannidis, P.; Ferrari, A.C.; di Carlo, A. Graphene-Based Interconnects for Stable Dye-Sensitized Solar Modules. *ACS Appl. Energy Mater.* **2021**, *4*, 98–110. [[CrossRef](#)]
59. Desilvestro, H.; Bertoz, M.; Tulloch, S.; Tulloch, G.E. Packaging, Scale-up, and Commercialization of Dye Solar Cells. In *Dye Sensitized Solar Cells*; Kalianasundaram, K., Ed.; CRC Press: Boca Raton, FL, USA, 2010; pp. 207–230.
60. Toyoda, T.S.; Nakajima, J.; Doi, S.; Fukumoto, S.; Ito, A.; Tohyama, T.; Yoshida, M.; Kanagawa, T.; Motohiro, T.; Shiga, T.; et al. Outdoor performance of large scale DSC modules. *J. Photochem. Photobiol.* **2004**, *164*, 203–207. [[CrossRef](#)]
61. Dai, S.; Weng, J.; Sui, Y.; Chen, S.; Xiao, S.; Huang, Y.; Kong, F.; Pan, X.; Hu, L.; Zhang, C.; et al. The design and outdoor application of dye-sensitized solar cells. *Inorg. Chim. Acta* **2008**, *361*, 786–791.
62. Fakharuddin, A.; Jose, R.; Brown, T.M.; Fabregat-Santiago, F.; Bisquert, J. A perspective on the production of dye-sensitized solar modules. *Energy Environ. Sci.* **2014**, *7*, 3952–3981. [[CrossRef](#)]

63. Mincuzzi, G.; Vesce, L.; Liberatore, M.; Reale, A.; di Carlo, A.; Brown, T.M. Laser-Sintered TiO<sub>2</sub> Films for Dye Solar Cell Fabrication: An Electrical, Morphological, and Electron Lifetime Investigation. *IEEE Trans. Electron Devices* **2011**, *58*, 3179–3188. [[CrossRef](#)]
64. Vesce, L.; Riccitelli, R. Processing and characterization of a TiO<sub>2</sub> paste based on small particle size powders for dye-sensitized solar cell semi-transparent photo-electrodes. *Prog. Photovoltaics Res. Appl.* **2011**, *20*, 960–966. [[CrossRef](#)]
65. Tagliaferro, R.; Colonna, D.; Brown, T.M.; Reale, A.; di Carlo, A. Interplay between transparency and efficiency in dye sensitized solar cells. *Opt. Express* **2013**, *21*, 3. [[CrossRef](#)] [[PubMed](#)]
66. Khenkin, M.V.; Katz, E.A.; Abate, A.; Bardizza, G.; Berry, J.J.; Brabec, C.; Brunetti, F.; Bulović, V.; Burlingame, Q.; Di Carlo, A.; et al. Consensus statement for stability assessment and reporting for perovskite photovoltaics based on ISOS procedures. *Nat. Energy* **2020**, *5*, 35–49. [[CrossRef](#)]
67. Calogero, G.; Barichello, J.; Citro, I.; Mariani, P.; Vesce, L.; Bartolotta, A.; di Carlo, A.; di Marco, G. Photoelectrochemical and spectrophotometric studies on dye-sensitized solar cells (DSCs) and stable modules (DSCMs) based on natural apocarotenoids pigments. *Dye. Pigment.* **2018**, *155*, 75–83. [[CrossRef](#)]
68. Castro-Hermosa, S.A.; Yadav, S.K.; Vesce, L.; Guidobaldi, A.; Reale, A.; Di Carlo, A.; Brown, T.M. Stability issues pertaining large area perovskite and dye-sensitized solar cells and modules. *J. Phys. D Appl. Phys.* **2016**, *50*, 3. [[CrossRef](#)]
69. Hinsh, A.; Kroon, J.M.; Kern, R.; Uhlendorf, I.; Holzbock, J.; Meyer, A.; Ferber, J. Long term stability of Dye Sensitized Solar Cells. *Prog. Photovolt. Res. App.* **2001**, *9*, 425–438. [[CrossRef](#)]
70. Djurišić, A.B.; Liu, F.; Ng, A.M.; Dong, Q.; Wong, M.K.; Ng, A.; Surya, C. Stability issues of the next generation solar cells. *Phys. Status Solidi (RRL)* **2016**, *10*, 281–299. [[CrossRef](#)]
71. Bari, D.; Wrachien, N.; Tagliaferro, R.; Penna, S.; Brown, T.M.; Reale, A.; di Carlo, A.; Meneghesso, G. Thermal stress effects on Dye-Sensitized Solar Cells (DSSCs). *Microelectron. Reliab.* **2011**, *51*, 1762–1766. [[CrossRef](#)]
72. Sauvage, F. A Review on Current Status of Stability and Knowledge on Liquid Electrolyte-Based Dye-Sensitized Solar Cells. *Adv. Chem.* **2014**, *2014*, 1–23. [[CrossRef](#)]
73. Kwak, C.H.; Baeg, J.H.; Yang, I.M.; Giribabu, K.; Lee, S.; Huh, Y.S. Degradation analysis of dye-sensitized solar cell module consisting of 22 unit cells for thermal stability: Raman spectroscopy study. *Sol. Energy* **2016**, *130*, 244–249. [[CrossRef](#)]